



Influence of electrolyte composition and temperature on behaviour of AB₅ hydrogen storage alloy used as negative electrode in Ni–MH batteries



Malgorzata Karwowska ^a, Tomasz Jaron ^b, Karol J. Fijalkowski ^b, Piotr J. Leszczynski ^b, Zbigniew Rogulski ^{a,b}, Andrzej Czerwinski ^{a,b,*}

^a Faculty of Chemistry, University of Warsaw, Pasteura 1, 02-093 Warsaw, Poland

^b Centre of New Technologies, University of Warsaw, Zwirki i Wigury 93, 02-089 Warsaw, Poland

HIGHLIGHTS

- The AB₅-type metal alloy (Mm–Ni_{4.1}Al_{0.2}Mn_{0.4}Co_{0.45}) has been investigated in alkali metals hydroxides solutions.
- Hydrogen diffusion coefficient has been determined using limited volume electrode (LVE) containing no binder additives.
- The unit cell of LaMmNi_{4.1}Al_{0.2}Mn_{0.4}Co_{0.45} have been refined in the Cu_{5.4}Yb_{0.8} structure type.

ARTICLE INFO

Article history:

Received 23 January 2014

Received in revised form

25 March 2014

Accepted 11 April 2014

Available online 24 April 2014

Keywords:

Ni–MH battery

AB₅ alloy

Hydrogen sorption

Diffusion coefficient

Limited volume electrode (LVE)

ABSTRACT

The AB₅-type metal alloy (Mm–Ni_{4.1}Al_{0.2}Mn_{0.4}Co_{0.45}) has been investigated in different electrolytes (LiOH, NaOH, KOH, RbOH, CsOH). All of the electrochemical measurements have been performed using limited volume electrode technique (LVE). Thickness of the working electrode is nearly equal to the diameter of the grain (ca. 50 µm). Hydrogen diffusion coefficient has been determined using chronoamperometry. Hydrogen diffusion coefficient calculated for 100% state of charge reaches maximum value in KOH ($D_H = 4.65 \cdot 10^{-10} \text{ cm}^2 \text{ s}^{-1}$). We have obtained the highest value of capacity for the electrode in KOH and the lowest – in CsOH. The temperature influence on alloy capacity has been also tested. The alloy has been also characterised with SEM coupled with EDS, TGA/DSC and powder XRD. The unit cell of MmNi_{4.1}Al_{0.2}Mn_{0.4}Co_{0.45} have been refined in the Cu_{5.4}Yb_{0.8} structure type (a modified LaNi₅ structure); the structure is unaffected by the electrochemical treatment.

© 2014 Elsevier B.V. All rights reserved.

1. Introduction

Nickel–metal hydride batteries are one of the most used electrochemical power sources. Ni–MH batteries are much less toxic than nickel–cadmium batteries and still much cheaper and safer than lithium-ion batteries. Although they are excellent for powering of many portable devices or Hybrid Electric Vehicles (HEV) [1–3], the attainable current densities of Ni–MH batteries are not sufficient for their use in the devices demanding very high power densities or for usage at low temperatures. Preparation of new

hydrogen storage alloys, used as the anode materials in Ni–MH batteries is one of the methods considered for the improvement of these batteries [4].

Limited Volume Electrode (LVE) technique is used to investigate hydrogen storage alloys. In case of powder hydrogen storage alloys LVE electrodes are prepared by a high-pressure compression. In our approach [5] we form a pellet of a pure alloy pressed in between two pieces of a gold mesh used as a current collector. We do not use any binders (i.e. PTFE, PVA, graphite, metal powders) which could influence the observed electrochemical behaviour of the alloy investigated [1,6–9].

In this paper we present and characterise a hydrogen storage AB₅-type metal alloy of a nominal composition: Mm–Ni_{4.1}Al_{0.2}Mn_{0.4}Co_{0.45}. The aims of our work were: (i) physicochemical characterisation of the Mm–Ni_{4.1}Al_{0.2}Mn_{0.4}Co_{0.45} hydrogen storage alloy, (ii) determination of electrochemical

* Corresponding author. Faculty of Chemistry, University of Warsaw, Pasteura 1, 02-093 Warsaw, Poland.

E-mail addresses: acerw@chem.uw.edu.pl, andrzej.a.czerwinski@gmail.com (A. Czerwinski).

capacity of the alloy in several 1 M alkali metal hydroxide electrolytes, (iii) investigation of hydrogen diffusion coefficient in the alloy using different electrolyte compositions.

2. Experimental

2.1. Preparation of limited volume electrode (LVE)

Limited Volume-type working electrodes were prepared by pressing a small amount (up to 30 mg) of an AB₅-type alloy (Mm–Ni_{4.1}Al_{0.2}Mn_{0.4}Co_{0.45}, prepared by mechanical milling) into an Au metal mesh (99.9%, Goodfellow, nominal aperture 0.25 mm) under pressure of up to 20 MPa [5]. We used gold matrix due to (i) electrochemical neutrality within wide potential window, (ii) chemical inertness in respect to hydrogen absorption processes, (iii) high electronic conductivity and (iv) softness and compressibility allowing pressing of the alloy particles into the net without damaging the structure of the formers.

The electrode was placed in a specially designed PTFE holder [5] (Fig. 1) similar to the one used by Zheng et al. [10]. We put the electrode between two pieces of separator (polyethylene) used in standard Ni–MH cells.

Such experimental setup allows us to measure the electrochemical response from the pure alloy material, as no binder additives are necessary.

2.2. Electrochemical setup and techniques

MH-LV electrodes were activated by 50 cycles in potential range between –1.1 and –0.4 V vs. Hg|HgO at 2 mV s^{–1}. The voltammetric (CV) and chronoamperometric (CA) measurements were performed with an AUTOLAB 30 (Eco Chemie B.V., The Netherlands) electrochemical analyzer. A scanning electron microscope (SEM) LEO 435VP coupled with an energy-dispersive X-ray spectroscopy (EDS) analyzer (Röntec EDR286) was used to investigate of the structure and elemental composition of the electrodes.

The temperature was stabilised using KRYO51 bath with a Lauda Proline 855 (Proline 855) thermostat.

All the measurements were performed in a three-electrode system in Teflon cell. MH-LVE electrode was used as a working electrode, Hg|HgO with 6 M KOH (HYDROMET, Poland) and gold sheet (Mint of Poland) served as reference and counter electrodes, respectively. All the potentials in this paper are referred to Hg|HgO.

2.3. Other techniques

Powder diffraction patterns (XRD) were recorded using Bruker D8 Discover and PANalytical X'Pert Pro diffractometers, with

Table 1

Amount [% weight] of the most abundant elements of the alloy determined by EDS for as synthesized alloy and after 6 months.

	La	Ce	Ni	Co	Mn	Al
EDS (as synthesized)	20.1	8.5	55.0	6.1	4.8	4.8
EDS (after 6 months)	19.91	7.80	56.94	5.75	4.08	2.00

CuK α_{12} ($\lambda \approx 1.5406 \text{ \AA}$) and CoK α_{12} ($\lambda \approx 1.78901 \text{ \AA}$) radiation, respectively. A parallel X-ray beam was used, with the $K_{\alpha 1}:K_{\alpha 2}$ intensity ratio of ca. 2:1. Samples were loaded into 0.3 mm thick quartz capillaries under air. To decrease absorption of radiation (high-density samples) only the walls of capillaries were covered with powder. Jana2006 [11] was used for Rietveld refinement of the structure model described in the following section. The shape of diffraction peaks was modelled by a pseudo-Voigt function and the anisotropic broadening as well as the preferred orientation (March–Dollase) corrections were used. The atomic displacement parameters (ADP) of lanthanides as well as ADP of non-lanthanide metals (M) were set equal. Due to unreliable refinement parameters, the independent coordinate of M at 2e Wyckoff site was fixed as $z = 0.3$. The final profile fit parameters are as follows: $R_p = 0.95\%$, $R_{wp} = 1.40\%$, GOF = 1.11, $R_{Bragg} = 4.24\%$. Further details of the crystal structure of Mm–Ni_{4.1}Al_{0.2}Mn_{0.4}Co_{0.45} alloy may be obtained from Fachinformationszentrum Karlsruhe, 76344 Eggenstein-Leopoldshafen, Germany (fax: (+49)7247-808-666; e-mail: crysdata@fizkarlsruhe.de) on quoting the CSD number 427242.

EDS measurements were performed to determine elemental composition of the alloy. EDS data was collected using FE-SEM Merlin form Zeiss.

Average diameter of the grains of the alloy was determined using Infrared Particle Sizer (IPS) device IPS UA from Kamika with detection limit of 0.5 μm . Measurements were performed in the range of 0–150 μm with the sensitivity of 0.5 μm .

Thermal stability of the alloy was investigated using an STA 409 simultaneous thermal analyzer from Netzsch, in the temperature range 0–550 °C. Simultaneous thermogravimetric analysis (TGA), differential scanning calorimetry (DSC) and evolved gas analysis (QMS) was done. The samples were loaded into alumina crucibles. High purity argon (99.9999%) was used as a carrier gas.

3. Results and discussion

3.1. Characterisation of the alloy

The amount of the most abundant elements of the alloy was determined with EDS (see Table 1). However, the amount of the least-abundant elements cannot be determined precisely with this

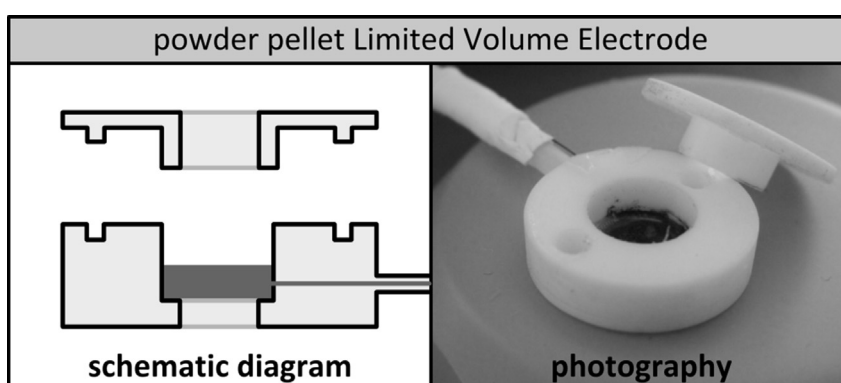


Fig. 1. Limited volume electrode made of hydrogen storage alloy powder pellet placed in a PTFE holder.

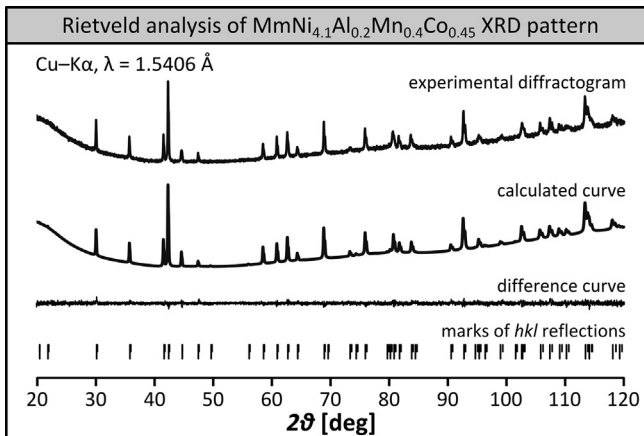


Fig. 2. Rietveld analysis of Mm–Ni_{4.1}Al_{0.2}Mn_{0.4}Co_{0.45} alloy (CuK α_{12}).

method due to an overlap of their signals with the signals of the most abundant elements and other limitations of EDS technique. Therefore we have used the nominal composition for the further considerations. From Table 1 it can be seen that the contents of the elements are different for as synthesized alloy and after 6 months. These EDS measurements differ and it is due to changes occurring during the time of storage the material. We explain it as the atom segregation within the alloy particles (this phenomenon was previously observed i.e. by Wallace et al. [12]). The EDS allows us to determine the composition of the surface layers of the alloy (up to few microns), so we cannot obtain the average content of every element in the alloy. One should also take under consideration that the alloy is composed of another elements also (vestigial amount of Pr, Nd, O, C etc.) which can disturb receiving proper results. The nominal stoichiometry was obtained from the weight of components used in high energy ball milling to obtain the alloy.

The powder X-ray diffraction pattern of the investigated alloy (Fig. 2) shows signals from a single phase, which are consistent with a hexagonal (P6/mmm) unit cell of CaCu₅ structure type adopted by native LaNi₅ [13,14]. The unit cell constants of Mm–Ni_{4.1}Al_{0.2}Mn_{0.4}Co_{0.45} are only slightly larger than those of LaNi₅ (ca. 1.4% greater volume): $a = b = 5.0079(5)$ Å, $c = 4.0521(4)$ Å, $V = 88.007(16)$ Å³.

While the diffraction pattern indicates the structure similar to that adopted by LaNi₅, the nominal stoichiometry of LnM_{5.25} (Ln = La, Ce, Nd, Pr, M = Ni, Co, Mn, Al), and the lack of diffraction signals from M (the expected contamination if the alloy crystallised as the LnM₅ compound) indicate that a modified structural model

would be more appropriate. Such a model based on Cu_{5.4}Yb_{0.8} structure type has been proposed by Percheron-Guégan et al. for LaNi_{5.12} and related compounds with the excess of metal M: Ln_{1-x}M_{5+2x} (Ln – lanthanide, M – transition metal or Al) [15]. In this structure, some of the lanthanide atoms at the cell origin (1a Wyckoff site) are replaced by a pair of M atoms at the 2e site (0,0, $\pm z$) and some of M atoms at the 2c site ($\frac{1}{3}, \frac{2}{3}, z$) move to the 6l site ($x, 2x, 0$).

The distribution of M atoms among various Wyckoff sites in the Ln_{1-x}M_{5+2x} alloys is typically nonuniform and it depends on the size and the electronic properties of a particular atom [15,16]. However, a reliable refinement of the occupancy in the multiple-substituted alloys requires several independent diffraction data sets. This could be achieved for multiwavelength synchrotron powder diffraction, with the use of anomalous dispersion effects [17]. Due to such limitations, we have assumed a nominal composition of the alloy investigated by us, and a uniform distribution of M atoms between the Wyckoff sites. The structure of the alloy remains unchanged after the electrochemical treatment.

Average grain size of the Mm–Ni_{4.1}Al_{0.2}Mn_{0.4}Co_{0.45} alloy was determined to be 48 µm (Figs. 3 and 4). The fraction of the smallest grains (10% of the population) is formed by the particles of the diameter up to 25 µm. 90% of the population are grains of the diameter not extending 76 µm.

Using IPS technique we have determined the average spherical coefficient of the grains of the alloy to be 1.146. The specific mass surface of the alloy is equal to 606 cm² g⁻¹, while specific volume surface of the alloy is equal to 1539 cm² cm⁻³. Effective surface of an average working electrode used in our electrochemical measurements was ca. 9.5 cm², while the surface of a solid electrode of the same geometry would not extend 1.6 cm².

The Mm–Ni_{4.1}Al_{0.2}Mn_{0.4}Co_{0.45} alloy is stable over the temperature range of 0–550 °C, no mass loss of the sample was detected. We have observed two endothermic events at 425 °C and 465 °C upon heating. These processes are reversible, i.e. during the cooling mode two exothermic events at the same temperatures appear. It might be melting of the alloy preceded by a crystal phase transition.

3.2. Influence of electrolyte composition on hydrogen sorption

We have performed a series of experiments using 1 M solutions of alkali metal bases: LiOH, NaOH, KOH, RbOH, CsOH. The same amount of electrolyte (40 cm³) was used every time. C.Z. Yu et al. proved that the amount of electrolyte has an influence on the electrode parameters [18]. We observed that the activation process plays an important role in MH-electrode preparation. It leads to oxide layer reduction and impurities removing from the surface.

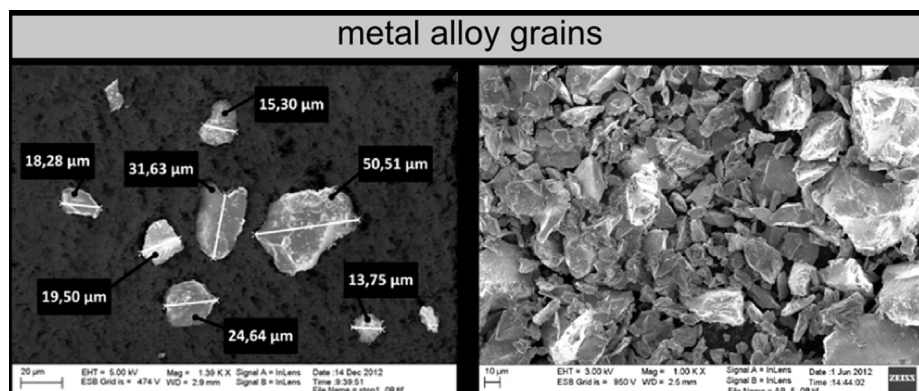


Fig. 3. SEM image of the metal alloy grains and the MH-electrode surface.

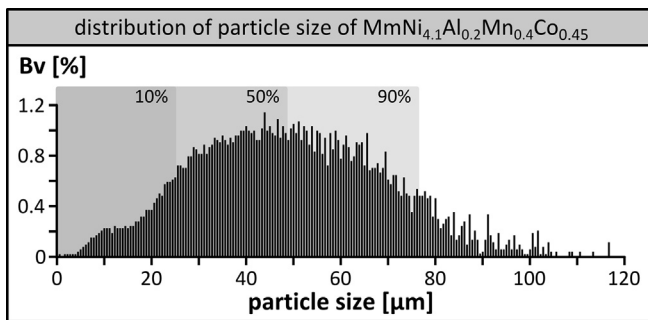


Fig. 4. Distribution of the particle size of the $\text{Mm}-\text{Ni}_{4.1}\text{Al}_{0.2}\text{Mn}_{0.4}\text{Co}_{0.45}$ alloy. Percentile values of 10%, 50% and 90% of the population exposed with grey fields. B_V – volume fraction [%]; sample population – 200,000 particles.

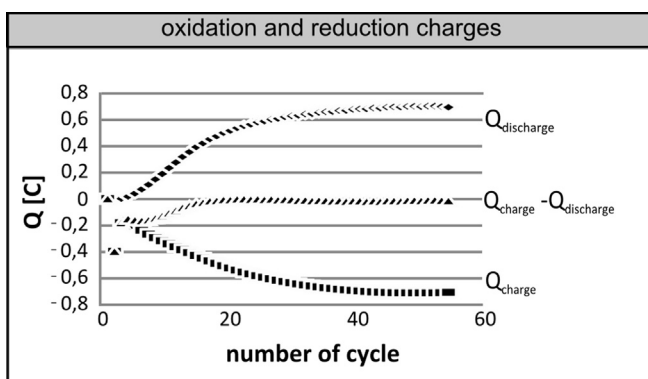


Fig. 5. Oxidation and reduction charges as a function of number of cycle.

The activation process causes real surface increase (we observed cracking of the grains). The oxidation and reduction charges reaches stable value after 40 cycles of voltammetry in all electrolytes used (Fig. 5). It is significant that the maximum capacity value is reached after 40 cycles in CV (0.002 V s^{-1}) and after that kind of activation – in the first step in CA.

The capacity of the alloy obtained in CV technique is lower than in CA (Figs. 6 and 7). These situation is due to non-equilibrium state during voltammetric measurements (with scanning rate $v = 0.002 \text{ V s}^{-1}$).

According to our results, the composition of the electrolyte significantly influences the electrochemical characteristics of the working electrode. The capacity value was obtained from charge of discharging electrode. The time required for full charge of electrode is dependent on the electrolyte composition.

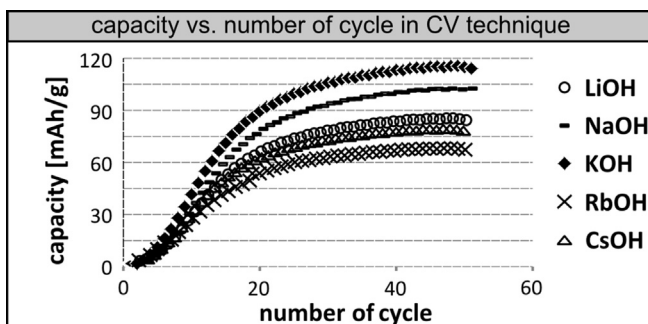


Fig. 6. Discharge capacity obtained in CV measurements in different solutions. Temperature $T = 293 \text{ K}$, scanning rate $v = 2 \text{ mV s}^{-1}$.

The capacity of the alloy is the highest in KOH solution, so the observed dependence is not linear in respect with ionic radius of the alkali metal cation (Fig. 7). The capacity values shown on Fig. 7 are results obtained in the first cycle of CA measurements (after full voltammetric activation).

We determined hydrogen diffusion coefficient (D_H) by charging and discharging working electrode maintaining constant current. The model of a finite space diffusion inside spherical particles was applied in the analysis of CA desorption curves [5,19]:

$$I = \left(6FD_H((c_0 - c_S)) / \delta d^2 \right) \exp \left(-\pi^2 D_H t / d^2 \right). \quad (1)$$

where F is Faraday constant (96485 C mol^{-1}), c_0 and c_S are bulk and surface hydrogen concentration, respectively, δ is the diffusion layer thickness, t is time and d is the radius of a single alloy particle. D_H value can be calculated from the slope of a linear part of $\ln I$ vs. time plot.

Fig. 8 presents D_H values obtained from CA measurements. D_H changes nonlinearly in the function of state of charge (SOC) in a similar way for all the investigated electrolytes. For the low values of SOC (lower than 0.2) D_H decrease steeply, for the higher values of SOC (over 0.2) changes of D_H are mild. We noticed that at room temperature D_H values in different alkali metal hydroxide electrolytes change in an order: $\text{LiOH} < \text{NaOH} < \text{KOH} > \text{RbOH} > \text{CsOH}$.

We observed that hydrogen diffusion coefficient (D_H) nonlinearly decreases with an increase of the state of charge (SOC) of the electrode and it depends on the electrolyte composition. Hydrogen diffusion coefficient is also related to the concentration of hydrogen in the material.

The differences in the values of hydrogen diffusion coefficient observed for different 1 M electrolytes suggest a strong impact of an electrolyte surface layer composition on the process of hydrogen diffusion in the bulk material. Even though the concentration of the solutions used in experiments are the same (so the H_2O and OH^- contents are the same) the results differs for different alkali metal hydroxide solutions. This is the evidence for statement that the solution composition influences the parameters of the metal alloy (capacity and the hydrogen diffusion coefficient in the alloy).

The influence of the alkali metal cations on hydrogen diffusion process taking place in the alloy particles can be explained by strong interaction of the metals or cations with the hydrogen absorbed. Intercalation of the alkali metal cations into/under the surface layer of the alloy particles is also probable [20]. Such intercalation might modify the properties of the alloy. Such a phenomenon was previously observed in Pd electrodes [21]. The presence of caesium metal inside palladium after hydrogen sorption from caesium hydroxide solution was proved by radiotracer method (Nuclear Activation Analysis) [22].

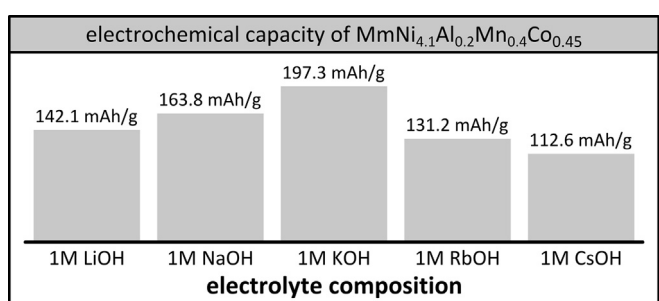


Fig. 7. Electrochemical capacity of the alloy as a function of composition of 1 M alkali metal hydroxide solution (maximum capacity value for each electrolyte, obtained in the 1st CA cycle after CV activation).

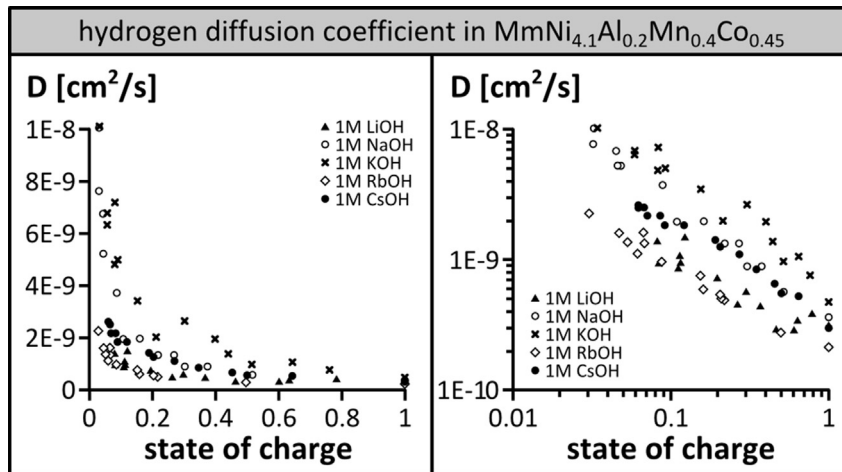


Fig. 8. Hydrogen diffusion coefficient as a function of composition of 1 M alkali metal hydroxide solution.

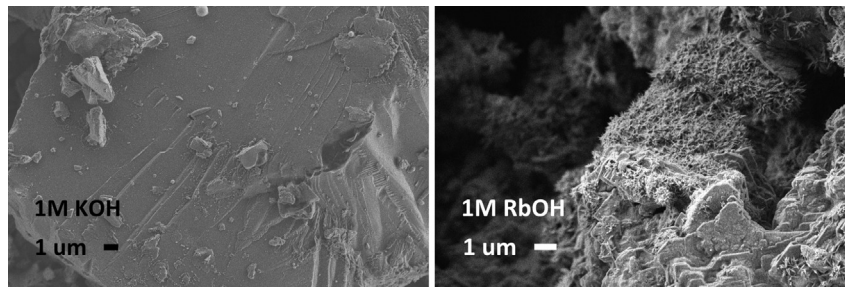


Fig. 9. SEM images of surface of electrode after CV and CA measurements (293 K) in KOH and RbOH. The structures of $Mm(OH)_x$ are visible (the needle shape).

As it is showed above the highest value of capacity of the alloy is related with the highest value of hydrogen diffusion coefficient and it is reached in 1 M KOH solution. This effects can be connected with the highest concentration of free spaces on the surface and inside the alloy at the presence of potassium cation in the solution. We can assume that there is a big role of a metal cations (or metals) absorption into the alloy structure. If we assume that metal cations can block the interstitial places, we should consider phenomenon caused by the intercalated metal (or metal cation – the nature of absorbed character is not known) related to the radius of the metal. We can assume that the bigger (with bigger atomic/cationic radius) atom (cation), the lower amount of the intercalated cation. So the cation with the lowest radius (Li^+) should block the most of interstitial places so the hydrogen cations cannot be absorbed. We can also suppose that alkali metal absorbed into the alloy may (locally) enlarge parameters of the unit cell. And then the relation considered should be: the bigger cation, the bigger changes and more (volumetric) place for hydrogen to be absorbed. So it suggests that the lowest blocking property have Cs^+ cations (and the hydrogen capacity of the alloy in $CsOH$ solution should be the highest). On the other hand, probably the amount of absorbed cations is connected with its radius – the bigger radius, the lower amount of absorbed metal. So the enlarging properties (and the highest hydrogen capacity) are stronger for Li^+ (because of the highest amount of absorbed Li). On the other hand we suggest that hydrides durability plays also an important role in observed effect. The most durable hydride (among alkali metal hydrides) is LiH and the least durable – CsH , so the absorbed lithium could make difficulties for hydrogen transport trough the alloy structure.

That can be one of the explanation of the alkali metal cations influencing the hydrogen absorption into the metal alloy and

the highest capacity of the alloy measured in KOH (due to the average atomic/cationic radius). It has to be noted that there is significant difference (ca. 15%) in hydrogen capacity electrochemically absorbed from the solution with and without alkali cations [23]. The influence of alkali metals on the hydrogen capacity of palladium has been also reported [21].

What is more the interaction between alkali metal cations and the surface of the material grains is probable. The corrosion process takes place during measurements (hydroxides and oxides are formed, i.e. $Mm(OH)_x$, $Co(OH)_2$, $Mn(OH)_2$). Amount of the corrosion products depends on the electrolyte. The strongest corrosion we observed in RbOH and $CsOH$. As it is seen on Fig. 9 the corrosion of

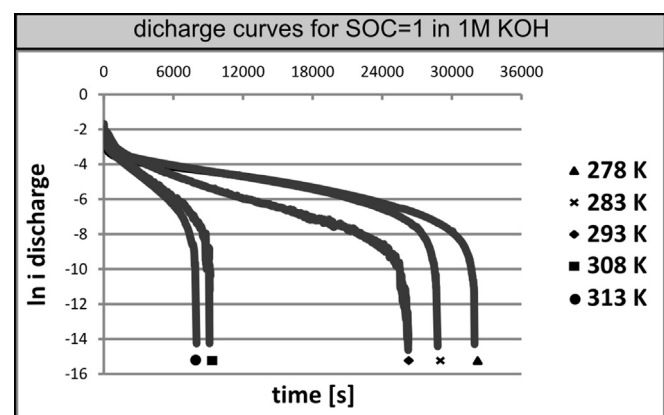


Fig. 10. The discharge curves as a function of time of discharge in different temperatures.

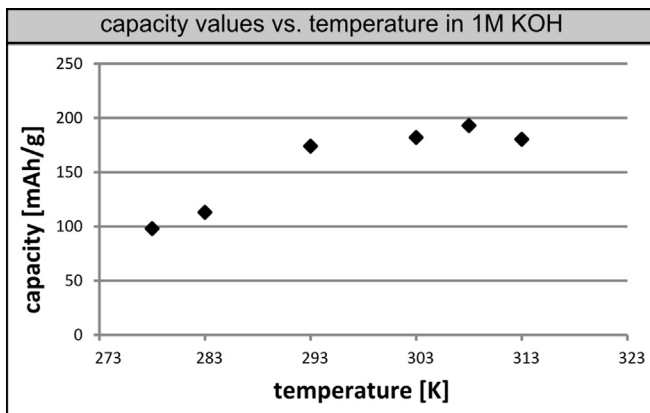


Fig. 11. Capacity (obtained in the 1st CA cycle after CV activation) of the alloy obtained in different temperatures in 1 M KOH.

the alloy is weaker when KOH solution is used. The highest corrosion processes we observed in RbOH (Fig. 9). The corrosion advancement we defined on the basis of surface covering by hydroxides and oxides crystals.

3.3. Influence of temperature on capacity of the MH electrode

Because of the highest value of capacity of the electrode in KOH electrolyte we have performed a series of experiments in different temperatures using Lauda thermostat. The temperature range chosen for these measurements was caused by the typical temperatures the Ni–MH batteries work in. The time required for hydrogen desorption from the electrode is longer in lower temperatures (Fig. 10). It suggests slower diffusion of the hydrogen through the alloy grains at lower temperatures. Additionally we suggest that it can be also due to the higher viscosity of the electrolyte at lower temperatures which has an impact on the diffusion of OH[−] anions and H₂O molecules within the solution.

The capacity of the electrode increases with temperature increase and it's almost stable above 293 K (Fig. 11). The capacity value does not increase with increasing temperature above 293 K. It is connected with maximum theoretical capacity (which for the examined material is not higher than 6H/M and depends on the stoichiometry of the hydrides used in calculation). Also the corrosion processes are stronger in higher temperature so the efficiency of the hydrogen absorption and desorption is not completed. The capacity value obtained at 273 K is just the half of the maximum value obtained at 313 K. The impact of temperature on the parameters of the electrode was observed by other groups for similar alloys [24–26].

4. Conclusions

We performed a physicochemical characterisation of a hydrogen storage powder alloy MmNi_{4.1}Al_{0.2}Mn_{0.4}Co_{0.45}. The properties of the material were carefully studied. The structure type of the unit cell was determined. The alloy crystallises in a hexagonal (P6/mmm) unit cell of Cu_{5.4}Yb_{0.8} structure type (a modified LaNi₅ structure). Powder samples of the alloy contain mostly grains of a diameter 20–80 μm, the average grain size of the alloy was determined to be 48 μm. The alloy is stable at room temperature and its crystal structure remains unchanged after the electrochemical treatment. Also the thermal stability of the material was

investigated and we concluded that it is stable in wide range of temperature (0–550 °C).

We investigated electrochemical capacity of the alloy and hydrogen diffusion coefficient as a function of an electrolyte composition at room temperature. We used LiOH, NaOH, KOH, RbOH and CsOH as electrolytes. These are comprehensive measurements inclusive all alkali metal hydroxides. We observed the highest capacity and D_H values in 1 M KOH solution. The decrease of the electrochemical capacity of the alloy observed in other electrolytes can be explained by strong interaction of the electrolyte with the surface of the alloy (alkali metals intercalation and corrosion).

The influence of temperature on capacity of the alloy is significant. The decrease of temperature causes decrease of the capacity value. The capacity value is almost stable above 293 K. This topic will be the theme of our next article.

The results obtained suggest that the properties of the electrode made of the hydrogen storage alloy (MmNi_{4.1}Al_{0.2}Mn_{0.4}Co_{0.45}) highly depend on the composition of the electrolyte. The presented electrochemical study is important in view of designing new electrolytes to be used in Ni–MH batteries.

Acknowledgements

This research was funded from 1552/B/H03/2011/40 and UMO-2011/01/B/ST4/00442 grants of the Polish National Centre of Science, and from 0122/IP3/2011/71 grant “Iuventus Plus” of the Polish Ministry of Science and Higher Education.

References

- [1] D. Linden, T.B. Reddy, *Handbook of Batteries*, third ed., McGraw-Hill, New York, 2002.
- [2] M.A. Fetzenko, S.R. Ovshinsky, B. Reichman, K. Young, C. Fierro, J. Koch, A. Zallen, W. Mays, T. Ouchi, *J. Power Sources* 165 (2007) 544.
- [3] C. Pillot, Main Trends for the Rechargeable Battery Market Worldwide 2007–2015, <http://www.avicenne.com>, #articles and presentations.
- [4] J. Kleperis, G. Wójcik, A. Czerwiński, J. Skowroński, M. Kopczyk, M. Bejtowska-Brezeńska, *J. Solid State Electrochem.* 5 (2001) 229.
- [5] Z. Rogulski, J. Dłubak, M. Karwowska, M. Krebs, M. Pytlak, E. Schmalz, A. Gumkowska, A. Czerwiński, *J. Power Sources* 195 (2010) 7517.
- [6] M. Geng, D.O. Northwood, *Int. J. Hydrogen Energy* 21 (1996) 887.
- [7] T. Ise, T. Murata, Y. Hirota, M. Nogami, S. Nakahori, *J. Alloys Compd.* 298 (2000) 310.
- [8] D.M. Kim, H. Lee, K. Cho, J.Y. Lee, *J. Alloys Compd.* 282 (1999) 261.
- [9] K. Naito, T. Matsunomi, K. Okuno, M. Matsuoka, C. Iwakura, *J. Appl. Electrochem.* 23 (1993) 1051.
- [10] G. Zheng, B.S. Haran, B.N. Popov, R.E. White, *J. Appl. Electrochem.* 29 (1999) 361.
- [11] V. Petricek, M. Dusek, L. Palatinus, *Jana2006. Structure Determination Software Programs*, Institute of Physics, Praha, Czech Republic.
- [12] W.E. Wallace, R.F. Karlceik, H. Imamura, *J. Phys. Chem.* 3 (1979) 1708.
- [13] H.N. Nowotny, *Z. Met.* 34 (1942) 247.
- [14] E.H. Kisi, C.E. Buckley, E.M. Gray, *J. Alloys Compd.* 185 (1992) 369.
- [15] A. Percheron-Guégan, C. Lartigue, J.C. Achard, P. Germi, F. Tasset, *J. Less-Common Met.* 74 (1980) 1.
- [16] M. Latroche, J.-M. Joubert, A. Percheron-Guégan, P.H.L. Notten, *J. Solid State Chem.* 146 (1999) 313.
- [17] J.M. Joubert, R. Černý, M. Latroche, A. Percheron-Guégan, K. Yvon, *J. Appl. Crystallogr.* 31 (1998) 327.
- [18] C.Z. Yu, G.J. Yan, W.H. Lai, Q.H. Dong, *J. Alloys Compd.* 293–295 (1999) 799.
- [19] X. Yuan, N. Xu, *J. Appl. Electrochem.* 31 (2001) 1033.
- [20] H. Uchida, K. Yamashita, M. Goto, *J. Alloys Compd.* 330–332 (2002) 622.
- [21] A. Czerwiński, I. Kiersztyn, M. Grdeń, *J. Solid State Electrochem.* 7 (2003) 321.
- [22] M. Czauderna, G. Maruszczak, A. Czerwiński, *J. Radioanal. Nucl. Chem. Lett.* 199 (1995) 375.
- [23] A. Czerwiński, R. Marassi, *J. Electroanal. Chem.* 322 (1992) 373.
- [24] C. Jeong, W. Chung, C. Iwakura, I. Kim, *J. Power Sources* 79 (1999) 19.
- [25] Y. Liu, H. Pan, M. Gao, Y. Zhu, Y. Lei, Q. Wang, *Electrochim. Acta* 49 (2004) 545.
- [26] A. Visintin, H.A. Peretti, C.A. Tori, W.E. Triaca, *Int. J. Hydrogen Energy* 26 (2001) 683.